# FCS experiments to quantify $Ca^{2+}$ diffusion and its interaction with buffers

Lorena Sigaut, Cecilia Villarruel, and Silvina Ponce Dawson

Citation: The Journal of Chemical Physics **146**, 104203 (2017); doi: 10.1063/1.4977586
View online: http://dx.doi.org/10.1063/1.4977586
View Table of Contents: http://aip.scitation.org/toc/jcp/146/10
Published by the American Institute of Physics

# FCS experiments to quantify $Ca^{2+}$ diffusion and its interaction with buffers

Lorena Sigaut, Cecilia Villarruel, and Silvina Ponce Dawson
*Departamento de Física, FCEN-UBA, and IFIBA, CONICET, Ciudad Universitaria, Pabellón I, 1428 Buenos Aires, Argentina*

(Received 16 September 2016; accepted 3 February 2017; published online 14 March 2017)

$Ca^{2+}$ signals are ubiquitous. One of the key factors for their versatility is the variety of spatio-temporal distributions that the cytosolic $Ca^{2+}$ can display. In most cell types $Ca^{2+}$ signals not only depend on $Ca^{2+}$ entry from the extracellular medium but also on $Ca^{2+}$ release from internal stores, a process which is in turn regulated by cytosolic $Ca^{2+}$ itself. The rate at which $Ca^{2+}$ is transported, the fraction that is trapped by intracellular buffers, and with what kinetics are thus key features that affect the time and spatial range of action of $Ca^{2+}$ signals. The quantification of $Ca^{2+}$ diffusion in intact cells is quite challenging because the transport rates that can be inferred using optical techniques are intricately related to the interaction of $Ca^{2+}$ with the dye that is used for its observation and with the cellular buffers. In this paper, we introduce an approach that uses Fluorescence Correlation Spectroscopy (FCS) experiments performed at different conditions that in principle allows the quantification of $Ca^{2+}$ diffusion and of its reaction rates with unobservable (non-fluorescent) $Ca^{2+}$ buffers. To this end, we develop the necessary theory to interpret the experimental results and then apply it to FCS experiments performed in a set of solutions containing $Ca^{2+}$, a single wavelength $Ca^{2+}$ dye, and a non-fluorescent $Ca^{2+}$ buffer. We show that a judicious choice of the experimental conditions and an adequate interpretation of the fitting parameters can be combined to extract information on the free diffusion coefficient of $Ca^{2+}$ and of some of the properties of the unobservable buffer. We think that this approach can be applied to other situations, particularly to experiments performed in intact cells. *Published by AIP Publishing.* [http://dx.doi.org/10.1063/1.4977586]

## I. INTRODUCTION

$Ca^{2+}$ signals are ubiquitous. They are involved in muscle movement, heart beat, neuronal communication, egg fertilization, and cell death among other processes.[1,2] The versatility of intracellular $Ca^{2+}$ signals relies on the variety of spatio-temporal distributions that the cytosolic $Ca^{2+}$ concentration can display.[3–6] Prolonged high elevations of free cytosolic $Ca^{2+}$ lead to cell death.[7] Thus, cells keep basal cytosolic $Ca^{2+}$ at very low levels. The signals are then constructed by means of local and transient elevations of the concentration that can eventually propagate throughout the cell.[8] The timing and the spatial range of the signals are thus key for the establishment of the consequent end responses.[9] The rate at which $Ca^{2+}$ ions diffuse in the cytosol is one of the main factors that determine these two aspects of the signals. The diffusion coefficient of $Ca^{2+}$ was estimated in cytosolic extracts more than twenty years ago using radioactive $Ca^{2+}$.[10] In spite of the importance of having reliable estimates of this coefficient obtained *in situ*, to the best of our knowledge, there has not been a direct estimation of $Ca^{2+}$ diffusion in intact cells using other techniques, such as Fluorescence Correlation Spectroscopy (FCS). One of the problems associated with quantifying $Ca^{2+}$ diffusion in intact cells is the presence of $Ca^{2+}$ buffers.[11] In fact the fastest way by which cells can reduce the free cytosolic $Ca^{2+}$ concentration is by means of buffers that bind $Ca^{2+}$ with diverse affinities and kinetics.[12,13] Buffers not only reduce the total free $Ca^{2+}$ concentration, they also change its dynamics and spatial range of variation.[14,15] Thus, the net transport of the ions is not purely diffusive. It is possible, however, to describe this transport in terms of *effective* diffusion coefficients that take into account both the *free* diffusion rate of the ions and the way it is affected by $Ca^{2+}$ buffering.[16] Here by *free diffusion* we mean the net transport of (dilute) solute particles that randomly change their direction of movement when they collide with solvent molecules and, in this way, perform a random walk.[17,18] Effective diffusion, on the other hand, involves both reacting and non-reacting collisions. Thus, effective diffusion coefficients depend on the concentration of the reactants and on their reaction rates.[16] Contrary to free diffusion coefficients, effective ones are not unique. In particular, there is one (which we call *collective*) that describes the rate at which concentration inhomogeneities spread out with time while there is another (which we call the *single molecule*) which is the one that enters the proportionality factor between the mean square displacement of a single particle and time.[16,19] When probing reaction-diffusion systems, optical techniques such as FCS or Fluorescence Recovery After Photobleaching (FRAP) most often give information on effective diffusion coefficients[20,21] unless very small volumes are observed.[22] In these cases, FRAP prescribes the single molecule coefficient[20] while FCS gives both the collective and the single molecule ones.[21] Having an underlying biophysical model is thus most relevant to interpret the meaning of the diffusion coefficients that are estimated with optical experiments.[19] Effective diffusion coefficients

are weighted averages of the free coefficients of the interacting species that depend on their concentrations and reaction rates. Thus, it is necessary to estimate concentrations and reaction rates in order to infer free from effective diffusion coefficients.[23]

FCS was introduced in Ref. 24 where an application to quantify the reaction rates of a bimolecular reaction was presented. The technique was subsequently applied to quantify diffusion and binding properties both *in vitro* and *in vivo*.[25–33] In FCS the fluorescence is collected from a relatively small volume and the auto-correlation function (ACF) of the fluorescence fluctuations about the fluorescence mean is computed. Fitting the ACF with a model, concentrations and transport and reaction rates can be estimated, depending on the time scales that characterize the underlying dynamics.[22,34] Technical advances allowed the introduction of several improvements.[26,35–38] In particular, being able to scan over the sample (as with a confocal microscope) or to separate the light coming from two chromophores allowed the introduction of different variations of the technique (Image Correlation Spectroscopy (ICS),[39] Image Cross Correlation Spectroscopy (ICCS), Raster image correlation spectroscopy (RICS),[40] Spatiotemporal Image Correlation Spectroscopy (STICS)[41] (dual color), Fluorescence Cross Correlation Spectroscopy (FCCS),[42,43] etc.) in some of which the correlation between the fluorescence coming from different spatial points is computed. Versions of ICS also exist in which, instead of scanning the sample, the data are acquired with a camera that produces two-dimensional images. The use of two-photon and of Total-Internal-Reflection-Fluorescence (TIRF) microscopy, on the other hand, allowed the reduction of the observation volume opening up new application possibilities.[37] This was further improved by the use of nanoparticles that enhance locally the illumination intensity,[44] of photoactivatable dyes which allowed the quantification of the dynamics of transcription,[45,46] and of faster detection capabilities that increased the throughput of the technique.[47,48] An important part of the method lies in the fitting of the ACF with a model function and in the subsequent use of the fitting parameters to quantify relevant biophysical quantities. The quantification of diffusion coefficients from correlation times requires an *a priori* calibration of the illuminated volume which is usually done using a probe whose free diffusion coefficient is previously known. Although these *a priori* estimates may be available for diffusion in aqueous solutions, knowing their values in the interior of cells is not that common. To what extent a calibration performed in solution can be applied to the analysis of FCS experiments done in other settings such as cells is somewhat debatable. In particular, the illuminated volumes may differ depending on the mismatch between the refractive indices of the sample and of the medium that the light transverses before reaching it.[49] The effect of this mismatch on the (erroneous) quantification of diffusion coefficients from FCS experiments has been studied[50,51] so that, in principle, it could be corrected. There is also the option of using dual-focus FCS[52] where the fluorescence coming from two focal (overlapping) regions is collected. The distance between the two regions can be known quite accurately and provides the length scale with which the diffusion coefficients can be derived from the correlation times. The application of the method, however, requires additional equipment that is not always available. Besides these calibration problems, another important aspect of the experiments is the way in which the fitting parameters are interpreted. To this end, having a biophysical model of the underlying dynamics is unavoidable. Counting with such a model was key to reconcile the apparently disparate estimates of the diffusion coefficient of the protein, bicoid, in *Drosophila melanogaster* embryos.[19]

As we have mentioned, in FCS and in all of its variants the auto-(or cross)correlation function of the fluorescence fluctuations is computed. These correlation functions are characterized by two main quantities: correlation times and the weight with which each correlation time enters the ACF. When there is a single freely diffusing fluorescent species, the ACF is characterized by only one correlation time: the free diffusion time across the observation volume. The total weight, on the other hand, is inversely proportional to the mean number of particles in the observation volume. When the fluorescent particles diffuse and react, the ACF is characterized by various correlation times. Depending on the characteristics of the system and on the observation volume size it is possible that each correlation time be determined by only a free diffusion or reaction time.[22] Most often this is not the case, so that each correlation time depends on several of the parameters that characterize the various processes that underlie the dynamics of the system (see, e.g., Refs. 21, 30, and 31). In the case of $Ca^{2+}$ and its dyes, this turns out to be an advantage. Namely, $Ca^{2+}$ distributions are observed indirectly by using fluorophores that change their optical properties when bound to $Ca^{2+}$. In particular, single wavelength $Ca^{2+}$ dyes,[53] as the ones we use in the present paper, increase their fluorescence intensity when bound to $Ca^{2+}$. Thus, FCS experiments performed in systems that use these fluorophores actually collect the light coming from the $Ca^{2+}$-bound dye molecules (and, to a less extent, from $Ca^{2+}$-free dye molecules as well). Given that dye molecules are much more massive than $Ca^{2+}$, it is reasonable to assume that their free diffusion coefficient is the same regardless of whether they are actually free or bound to $Ca^{2+}$. Thus, if the observation volume were small enough, most likely dye molecules would transverse it without binding/unbinding to/from $Ca^{2+}$ so that the correlation time would only depend on the free diffusion coefficient of the dye molecules (which is the same in their free and $Ca^{2+}$-bound forms). No information on the transport of $Ca^{2+}$ ions would then be contained in the ACF. If the volume is larger so that several binding/unbinding $Ca^{2+}$-dye reactions occurred, the correlation times would be more complicated than before but would also depend on the free diffusion coefficient of $Ca^{2+}$, on the $Ca^{2+}$ and dye concentrations, and on the rates of their reaction. We have recently used this property to show that it is in fact possible to estimate the $Ca^{2+}$ free diffusion coefficient from sets of FCS experiments performed with $Ca^{2+}$ and varying concentrations of a single wavelength dye.[23] In the present paper, we go a step further. In particular, we study the ACF that can be obtained from FCS experiments performed in systems with $Ca^{2+}$, a $Ca^{2+}$ dye, and an (invisible) $Ca^{2+}$ buffer that competes with the dye for $Ca^{2+}$. The aim is to determine in which circumstances it is possible to quantify the diffusion rates of $Ca^{2+}$

and of the non-fluorescent buffer from the analysis of the $Ca^{2+}$-bound dye fluorescence fluctuations in such a case. In order to advance in this regard, we first study theoretically the various time scales that characterize this reaction-diffusion system and relate them with those that are encountered in the system with $Ca^{2+}$ and the $Ca^{2+}$ dye or with the other (non-fluorescent) buffer. We then obtain the Auto-Correlation Function (ACF) of the $Ca^{2+}$-bound dye fluorescence fluctuations for such a system. We subsequently present the results of a series of FCS experiments performed in aqueous solutions containing the dye Fluo-4 dextran, the $Ca^{2+}$ buffer EGTA, and different concentrations of $Ca^{2+}$. The analysis of the experiments shows that information on the concentration, $Ca^{2+}$ dissociation constant, and diffusion coefficient of the non-fluorescent buffer (EGTA) can in fact be obtained. In doing so, we also derive the $Ca^{2+}$ and dye free diffusion coefficients and the on- and off-rates of their interaction. As stated in Ref. 54, there is more information in most optical experiments than usually exploited and despite the limitations imposed by physics[55] there is still room for the development of novel analyses of FCS experiments to quantify various biological processes.[56] In particular, thanks to these developments, FCS "is emerging as a valid alternative" to quantify single-molecule dynamics in living cells without the need of actually observing individual molecules.[57] Our approach may be viewed as a contribution in this direction. Given that cells contain various different endogenous buffers, this study provides ideas on how to advance towards the quantification *in situ* of the transport and buffering properties of $Ca^{2+}$ in cells. In view of the recent results[58] on the effective diffusion rate of $IP_3$, a co-agonist of $Ca^{2+}$ for the activation of the receptors that are most often involved in intracellular $Ca^{2+}$ signals, the need to obtain such an estimate is ever more necessary.[59] We briefly discuss later how the approach introduced in this paper could be applied in intact cells.

## II. THEORY: REACTION-DIFFUSION SYSTEM WITH $Ca^{2+}$, A $Ca^{2+}$-DYE, AND ONE TYPE OF $Ca^{2+}$-BUFFER

We consider a system with $Ca^{2+}$, a single-wavelength $Ca^{2+}$-dye (Fluo-4), and another buffer. This is the simplest model that can mimic what occurs in real cells where there are actually several endogenous buffers that could trap $Ca^{2+}$. Thus, any experiment in which $Ca^{2+}$-diffusion is studied in intact cells will have to deal with the competition between the dye and the endogenous buffers. This system models the situation presented in this paper of FCS experiments performed in solutions containing $Ca^{2+}$ (Ca), Fluo-4 (F4), and EGTA (E). We assume that $Ca^{2+}$, the dye, F4, and the buffer or chelator, E, interact according to the following reaction schemes:

$$\mathrm{Ca} + \mathrm{F4} \underset{k_{on\mathrm{F4}}}{\overset{k_{off\mathrm{F4}}}{\leftrightarrows}} \mathrm{CaF4}, \tag{1}$$

$$\mathrm{Ca} + \mathrm{E} \underset{k_{on\mathrm{E}}}{\overset{k_{off\mathrm{E}}}{\leftrightarrows}} \mathrm{CaE}, \tag{2}$$

where CaF4 and CaE denote the $Ca^{2+}$-bound dye and chelator, respectively, and $k_{on}$ and $k_{off}$ are the on- and off-rates. We assume that $Ca^{2+}$ diffuses with the free coefficient, $D_{\mathrm{Ca}}$, that the dye both free and $Ca^{2+}$-bound diffuses with the free coefficient, $D_{\mathrm{F4}}$, and that the free and $Ca^{2+}$-bound buffers diffuse with the free coefficient, $D_{\mathrm{E}}$. Thus, the evolution equations that describe the dynamics of this system are given by

$$\frac{\partial[\mathrm{Ca}]}{\partial t} = D_{\mathrm{Ca}}\nabla^2[\mathrm{Ca}] - k_{on\mathrm{F4}}[\mathrm{Ca}]\,[\mathrm{F4}] + k_{off\mathrm{F4}}[\mathrm{CaF4}] - k_{on\mathrm{E}}[\mathrm{Ca}]\,[\mathrm{E}] + k_{off\mathrm{E}}[\mathrm{CaE}], \tag{3}$$

$$\frac{\partial[\mathrm{F4}]}{\partial t} = D_{\mathrm{F4}}\nabla^2[\mathrm{F4}] - k_{on\mathrm{F4}}[\mathrm{Ca}]\,[\mathrm{F4}] + k_{off\mathrm{F4}}[\mathrm{CaF4}], \tag{4}$$

$$\frac{\partial[\mathrm{CaF4}]}{\partial t} = D_{\mathrm{F4}}\nabla^2[\mathrm{CaF4}] + k_{on\mathrm{F4}}[\mathrm{Ca}]\,[\mathrm{F4}] - k_{off\mathrm{F4}}[\mathrm{CaF4}], \tag{5}$$

$$\frac{\partial[\mathrm{E}]}{\partial t} = D_{\mathrm{E}}\nabla^2[\mathrm{E}] - k_{on\mathrm{E}}[\mathrm{Ca}]\,[\mathrm{E}] + k_{off\mathrm{E}}[\mathrm{CaE}], \tag{6}$$

$$\frac{\partial[\mathrm{CaE}]}{\partial t} = D_{\mathrm{E}}\nabla^2[\mathrm{CaE}] + k_{on\mathrm{E}}[\mathrm{Ca}]\,[\mathrm{E}] - k_{off\mathrm{E}}[\mathrm{CaE}], \tag{7}$$

where we have used mass action kinetics to describe the reactions.

### A. Linear equations and effective diffusion coefficients

The computation of the Auto-Correlation Function (ACF) of the fluorescence fluctuations as done in Refs. 21, 22, 34, and 60 involves starting with the approximation to the master equation given by Eqs. (3)–(7) and then linearizing these equations around the equilibrium solution, $\mathrm{Ca}_{eq}$, $\mathrm{F4}_{eq}$, $\mathrm{CaF4}_{eq}$, $\mathrm{E}_{eq}$, $\mathrm{CaE}_{eq}$ that satisfies

$$\mathrm{Ca}_{eq}\,\mathrm{F4}_{eq} = K_{d\mathrm{F4}}\mathrm{CaF}\,4_{eq}, \quad \mathrm{Ca}_{eq}\,\mathrm{E}_{eq} = K_{d\mathrm{E}}\,\mathrm{CaE}_{eq}, \tag{8}$$

where $K_{d\mathrm{F4}} \equiv k_{off\mathrm{F4}}/k_{on\mathrm{F4}}$ and $K_{d\mathrm{E}} \equiv k_{off\mathrm{E}}/k_{on\mathrm{E}}$ are the dissociation constants of the reactions (1) and (2), respectively. In order to find the solutions of the linear system, we transform the equations to Fourier space.

The dynamics is then described by 5 branches of eigenvalues that depend on the wavenumber, $\mathbf{q}$, the variable conjugate to the position, $\mathbf{r}$, in Fourier space. Two of the branches correspond to the free diffusion of Fluo-4 and of EGTA, respectively, and are given by

$$\lambda_1 = -D_{\mathrm{F4}}q^2, \tag{9}$$

$$\lambda_2 = -D_{\mathrm{E}}q^2, \tag{10}$$

where $q = |\mathbf{q}|$. In order to interpret the meaning of the other three eigenvalues, we proceed as in Refs. 16 and 21 and expand their expressions up to order $q^2$. This expansion describes correctly the asymptotic approach to equilibrium and is valid earlier on if reactions occur on a faster time scale than diffusion[21,22] (in the fast reaction limit). In this way we obtain

$$\lambda_3 = -D_{ef1}q^2, \tag{11}$$

$$\lambda_4 = -\nu_{ef2} - D_{ef2}q^2, \tag{12}$$

$$\lambda_5 = -\nu_{ef3} - D_{ef3}q^2, \tag{13}$$

where $D_{ef1}$, $D_{ef2}$, and $D_{ef3}$ are *effective diffusion coefficients*. $D_{ef1}$ has a simple analytic expression

$$D_{ef1} = \frac{D_{\rm Ca} + x_{\rm F} D_{\rm F4} + x_{\rm E} D_{\rm E}}{1 + x_{\rm F} + x_{\rm E}}, \tag{14}$$

where $x_{\rm F} = {\rm F4}_{eq}^2/(K_{d\rm F4}{\rm F4}_{tot})$ and $x_{\rm E} = {\rm E}_{eq}^2/(K_{d\rm E}{\rm E}_{tot})$ with ${\rm F4}_{tot}$ and ${\rm E}_{tot}$ the total concentrations of the dye and chelator, respectively. Eq. (14) coincides with the expression derived in the rapid buffering approximation when there is more than one $Ca^{2+}$ buffer.[61,62] It is also the natural extension of the collective diffusion coefficient introduced in Ref. 16 for the case with more than one buffer. The analytic expressions of $D_{ef2}$, $D_{ef3}$, $\nu_{ef2}$, and $\nu_{ef3}$ are very long (see the Appendix). It is worth noticing that $D_{ef2}$ and $D_{ef3}$, differently from $D_{ef1}$, depend on the ratio $k_{\rm E} = k_{off\,\rm E}/k_{off\,\rm F4}$. It is also important to point out that the various coefficients satisfy the following relations:

$$D_{ef1} + D_{ef2} + D_{ef3} = D_{\rm Ca} + D_{\rm F4} + D_{\rm E}, \tag{15}$$

$$\nu_{ef2} + \nu_{ef3} = \nu_{\rm F4} + \nu_{\rm E}, \tag{16}$$

where $\nu_{\rm F4} = k_{off\,\rm F4}({\rm F4}_{eq}/K_{d\rm F4} + {\rm F4}_{tot}/{\rm F4}_{eq})$ and $\nu_{\rm E} = k_{off\,\rm E}$ $({\rm E}_{eq}/K_{d\rm E} + {\rm E}_{tot}/{\rm E}_{eq})$ are related to the inverse reaction time scales of $Ca^{2+}$ and F4 (in the absence of EGTA) and of $Ca^{2+}$ and EGTA (in the absence of F4), respectively. Namely, if we set $\nu_{\rm E} = 0 = x_{\rm E}$ in Eqs. 11–16, the resulting $\lambda_1$, $\lambda_3$, and $\lambda_4$ are the three eigenvalues that rule the dynamics of the linear problem in a system with $Ca^{2+}$ and the dye, F4.[23] As shown in Sec. II B, fluctuations in the $Ca^{2+}$-bound dye concentration decay with time scales that depend on all these effective diffusion coefficients and reaction rates. Part of the work presented in this paper is aimed at extracting $D_{\rm Ca}$, $D_{\rm E}$, and other E properties from these "mixed" characteristic times.

In order to illustrate how the various diffusion coefficients vary with the concentrations, we show in Figs. 1(a)–1(c) the ratios (with respect to $D_{\rm Ca}$) of the coefficients defined in Eqs. 11–13 as functions of the total $Ca^{2+}$ concentration, ${\rm Ca}_{tot}$. The figures were made using similar reaction parameters to those that we expect *a priori* (see Table II) for the reactions of $Ca^{2+}$ with Fluo-4 and EGTA. Regarding the free diffusion coefficients of the dye and the chelator, previous estimates indicate that EGTA diffuses faster than Fluo-4. Although the dissociation constants are known, reliable values of the individual on and off rates are not usually available. For this reason in Figs. 1(a)–1(c) we also explore in which way the different coefficients vary when the off-rates ratio, $k_{\rm E}$, is changed. We can observe that for all the conditions presented in Fig. 1, $D_{ef1} \to D_{\rm Ca}$ as ${\rm Ca}_{tot}$ is increased while $D_{ef2}$ and $D_{ef3}$ either approach $D_{\rm F4}$ or $D_{\rm E}$ depending on $K_{\rm E}$. We also show in the figure the ratio with respect to $D_{\rm Ca}$ of the two effective diffusion coefficients that are obtained in a system with $Ca^{2+}$ and only one buffer, $B$, (either $B = {\rm F4}$ or $B = {\rm E}$) which are given by

$$D_{ef1}^{\rm Ca–B} = \frac{D_{\rm Ca} + x_B D_B}{1 + x_B}, \tag{17}$$

$$D_{ef2}^{\rm Ca–B} = \frac{x_B D_{\rm Ca} + D_B}{1 + x_B}, \tag{18}$$

with $x_B = B_{eq}^2/(K_{dB}B_{tot})$.

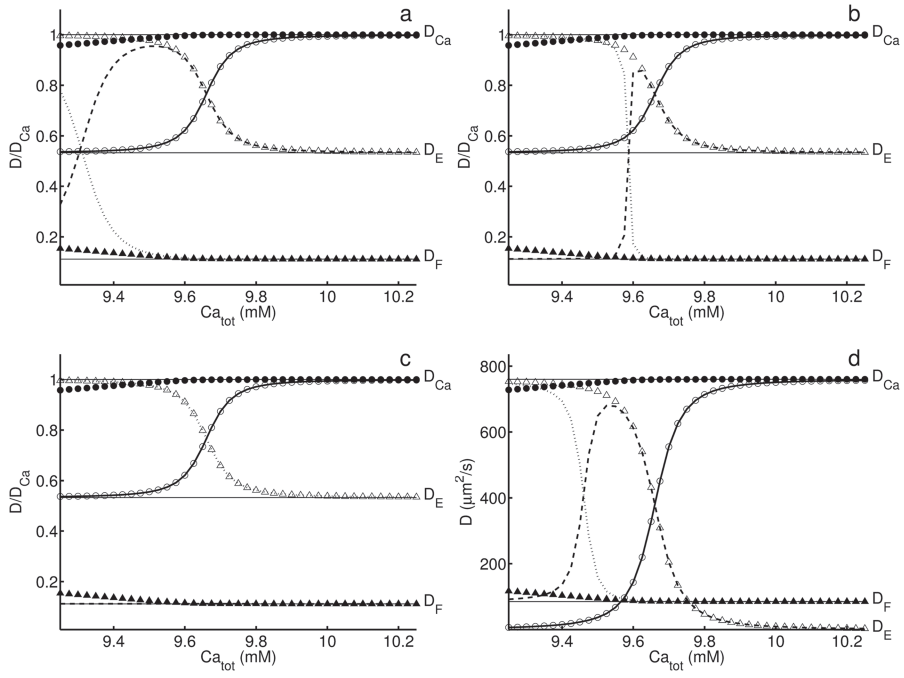


FIG. 1. Ratios, with respect to the free diffusion coefficient of $Ca^{2+}$, of the three effective diffusion coefficients, $D_{ef1}$ (solid line), $D_{ef2}$ (dotted line), and $D_{ef3}$ (dashed line), of the system formed by $Ca^{2+}$, Fluo-4, and EGTA as functions of the total $Ca^{2+}$ concentration. Plots of the two effective diffusion coefficients of the system with $Ca^{2+}$ and Fluo-4, $D_{ef1}^{\rm Ca–F4}$ (black circle) and $D_{ef2}^{\rm Ca–F4}$ (black triangle) and of the system with $Ca^{2+}$ and EGTA, $D_{ef1}^{\rm Ca–E}$ (open circle) and $D_{ef2}^{\rm Ca–E}$ (open triangle). The corresponding ratios of the free diffusion coefficients are indicated with horizontal lines (thin solid curve). All plots were done with $D_{\rm Ca} = 760\ \mu{\rm m}^2/{\rm s}$, $D_{\rm F4} = 85\ \mu{\rm m}^2/{\rm s}$, ${\rm F4}_{tot} = 676$ nM, ${\rm E}_{tot} = 9.66$ mM, $K_{d\rm F4} = 2600$ nM, and $K_{d\rm E} = 150$ nM. In (a)–(c) we used $D_{\rm E} = 405\ \mu{\rm m}^2/{\rm s}$, $k_{off\,\rm E} = 1\ {\rm s}^{-1}$ and $k_{\rm E} = 0.001$, $k_{off\,\rm F4} = 1000\ {\rm s}^{-1}$ (a); $k_{\rm E} = 0.01$, $k_{off\,\rm F4} = 100\ {\rm s}^{-1}$ (b); $k_{\rm E} = 0.1$, $k_{off\,\rm F4} = 10\ {\rm s}^{-1}$ (c). In (d) we used $k_{off\,\rm F4} = 300\ {\rm s}^{-1}$, $k_{off\,\rm E} = 0.75\ {\rm s}^{-1}$, and $D_{\rm E} = 0\ \mu{\rm m}^2/{\rm s}$. We expect the latter choice to be closer to the situation we may encounter in an FCS experiment in intact cells.

The possibility of describing the coefficients for the case with two buffers, in terms of those obtained for the case with only one, also depends on the relative concentrations. In particular, if the total concentrations of chelator and $Ca^{2+}$ are in excess with respect to the indicator, F4 (the situation that we expect to encounter in the interior of a cell where small amounts of dye are added), it is

$$x_F \equiv \frac{F4_{eq}^2}{K_{dF4}F4_{tot}} \ll x_E \equiv \frac{E_{eq}^2}{K_{dE}E_{tot}}, \tag{19}$$

from which we obtain

$$D_{ef1} \approx \frac{D_{Ca} + x_E D_E}{1 + x_E} = D_{ef1}^{Ca-E}, \quad \text{if } x_F \ll x_E. \tag{20}$$

This can be seen in all the cases presented in Fig. 1, where $D_{ef1} = D_{ef1}^{Ca-E}$ for all the $Ca^{2+}$ concentrations probed. Whether the other effective coefficients can be approximated by those obtained in the systems with only one buffer also depends on the ratio of unbinding rates, $k_E = k_{off\,E}/k_{off\,F4}$. If $k_E > K_{dE}/K_{dF4}$ as in Fig. 1(c), it is $D_{ef2} = D_{ef2}^{Ca-E}$ and $D_{ef3} = D_{F4}$ for all the probed values of $Ca_{tot}$. If $k_E < K_{dE}/K_{dF4}$ as in Figs. 1(a) and 1(b), it is $D_{ef3} \approx D_{ef2}^{Ca-E}$ and $D_{ef2} \approx D_{F4}$ for large enough $Ca_{tot}$ ($Ca_{tot} > 9.6$ mM in our case). Under the latter condition, the behavior of $D_{ef3}$ can be derived from the expressions of the effective coefficients of the systems with $Ca^{2+}$ and the buffer, E. This can readily be deduced taking into account Eq. (20) and the equality $D_{ef1} + D_{ef2} + D_{ef3} = D_{Ca} + D_{F4} + D_E$ that always holds. Thus, if $D_{ef2} \approx D_{F4}$ we can conclude that $D_{ef3} \approx D_{Ca} + D_E - D_{ef1}$. Inserting this equality into Eq. (20), we obtain

$$D_{ef3} \approx \frac{x_E D_{Ca} + D_E}{1 + x_E} = D_{ef2}^{Ca-E}, \quad \text{if } x_F \ll x_E. \tag{21}$$

This is interesting because, if the ACF of the fluorescence fluctuations depends on the time scale associated with $D_{ef3}$ (something we deduce in Subsection II B), it means that it is possible to determine the properties of non-fluorescent $Ca^{2+}$ traps from FCS experiments using small amounts of $Ca^{2+}$ dye. This opens up the possibility of applying the strategy presented here to analyze $Ca^{2+}$ transport and buffering in cells. With this application in mind, we show in what follows experimental results that use this property of the autocorrelation times. Fig. 1(d) serves to illustrate what we expect to find in these experiments and in those that may be performed in intact cells. The effective diffusion coefficients displayed in it were obtained using the parameters that we think describe the experiments of the current paper (listed in Table II) with the exception of $D_E$ that we set equal to 0. In spite of this difference, the curves for $D_E = 0$ or $D_E$ as in Table II are qualitatively similar. Thus, we expect the various effective diffusion coefficients that characterize the system explored experimentally to have a clearly distinct behavior as $Ca_{tot}$ is varied and to be easily identifiable with those of the $Ca^{2+}$ and one buffer cases for certain ranges of $Ca_{tot}$. We decided to illustrate the $D_E = 0$ case in Fig. 1(d) because we expect it to be closer to the situation that may be encountered in intact cells with E representing an immobile endogenous buffer. Based on this figure, we then discuss how to derive the properties of endogenous $Ca^{2+}$ buffers in intact cells using FCS.

### B. Theoretical derivation of the auto-correlation function

The autocorrelation function (ACF) of the fluorescence fluctuations is defined and computed as

$$G(\tau) \equiv \frac{\langle \delta F(t) \delta F(t+\tau) \rangle}{\langle F(t) \rangle^2}, \tag{22}$$

where $\delta F(t) = F(t) - \langle F \rangle$ is the deviation of the fluorescence, F, from its mean, $\langle F \rangle$, which is approximated by the time average. For the problem at hand, we assume that only the $Ca^{2+}$-bound dye molecules are fluorescent. The dye molecules are fluorescent also in their $Ca^{2+}$-free form but with an intensity that is ~40 times smaller than that when bound to $Ca^{2+}$. As we discuss later, for our experimental conditions we estimate that the error that we introduce by neglecting the contribution of the free dye molecules to the ACF is less than 1%. Under this approximation, the fluorescence collected by the microscope at time $t$ is

$$F(t) = \Delta t \int d^3\vec{r} I(\vec{r}) Q [CaF4](\vec{r}, t), \tag{23}$$

where $\Delta t$ is the sampling time, $Q$ is the product of the absorption cross section by the fluorescence quantum yield and the efficiency of the fluorophore, and $I(\vec{r}) = \exp(-\frac{2(x^2+y^2)}{w_r^2} - \frac{2z^2}{w_z^2})$ takes into account the form of the illumination/detection profile of the microscope with $w = w_z/w_r$ the ratio of its widths in the axial, $w_z$, and perpendicular directions, $w_r$, respectively. Eq. (23) implies that $G(\tau)$ depends on the fluctuations in the number of $Ca^{2+}$-bound dye molecules in the observation volume, $V_{ef} = \pi^{3/2} w_r^2 w_z$. Assuming that the fluctuations are correctly described by the solutions of the linear version of Eqs. (3)–(7) as done in Ref. 60, it is possible to write $G(\tau)$ as an integral over the wavenumber, $\mathbf{q}$, introduced previously that depends on the various branches of eigenvalues of the linear problem. Expanding these expressions up to order $q^2$ as done before with the eigenvalues and following the same steps as described in Ref. 21, we obtain

$$G(\tau) = \frac{Go_{F4}}{\left(1 + \frac{\tau}{\tau_{D_{F4}}}\right)\sqrt{1 + \frac{\tau}{w^2 \tau_{D_{F4}}}}} + \frac{Go_{ef1}}{\left(1 + \frac{\tau}{\tau_{D_{ef1}}}\right)\sqrt{1 + \frac{\tau}{w^2 \tau_{D_{ef1}}}}} + \frac{Go_{ef2}\, e^{-\nu_{ef2}\tau}}{\left(1 + \frac{\tau}{\tau_{D_{ef2}}}\right)\sqrt{1 + \frac{\tau}{w^2 \tau_{D_{ef2}}}}} + \frac{Go_{ef3}\, e^{-\nu_{ef3}\tau}}{\left(1 + \frac{\tau}{\tau_{D_{ef3}}}\right)\sqrt{1 + \frac{\tau}{w^2 \tau_{D_{ef3}}}}}, \tag{24}$$

where $\tau_{D_{efi}} = \frac{w_r^2}{4D_{efi}}$ with $D_{efi}$ and $\nu_{efi}$ the parameters that characterize the eigenvalue branches given by Eqs. 11–13. Thus, the ACF is the sum of 4 components: two of them purely diffusive and the other two with exponential factors as well. As in the case of a single buffer, the first term in Eq. (24) corresponds to the free diffusion coefficient of the dye.[23] This term is exact and its weight is given by

$$Go_{F4} = \frac{1}{V_{ef} F4_{tot}}. \tag{25}$$

We do not have closed analytic expressions for the weights of the other components each of which is characterized by one of the effective diffusion coefficients, $D_{ef1}$, $D_{ef2}$, and $D_{ef3}$, described before. It is possible to show, however, that the sum of all the weights is inversely proportional to the concentration of fluorescent particles

$$Go_{tot} = \frac{1}{V_{ef}\mathrm{CaF4}_{eq}}. \tag{26}$$

This relationship follows from the fact that $Go_{tot} = G(\tau = 0)$ is the ratio between the variance, $\mathrm{var}(N_{\mathrm{CaF4}})$, and the square of the mean, $\langle N_{\mathrm{CaF4}}\rangle^2$, of the number of fluorescence particles, $N_{\mathrm{CaF4}}$, in the observation volume. Following,[60] all computations are done assuming that $N_{\mathrm{CaF4}}$ obeys Poisson statistics so that $G(0) = 1/\langle N_{\mathrm{CaF4}}\rangle$. This property also allows us to estimate the error we make by not considering the fluorescence coming from the $Ca^{2+}$-free dye molecules, $N_{\mathrm{F4}}$. Namely, assuming that the total number of dye molecules in the observation volume, $N_T$, is Poisson distributed and that, given a value of $N_T$, $N_{\mathrm{CaF4}}$ and $N_{\mathrm{F4}}$ are binomial[34] with $\langle N_{\mathrm{CaF4}}\rangle/\langle N_T\rangle = \mathrm{CaF4}_{eq}/\mathrm{F4}_{tot} = 1-\langle N_{\mathrm{F4}}\rangle/\langle N_T\rangle$, the ratio between the variance and the mean square fluorescence is $(\langle N_{\mathrm{CaF4}}\rangle + q^2\langle N_{\mathrm{F4}}\rangle)/(\langle N_{\mathrm{CaF4}}\rangle + q\langle N_{\mathrm{F4}}\rangle)^2$, where $q$ is the ratio of the molecular brightness of the free over that of the $Ca^{2+}$-bound dye molecules ($q \sim 1/40$). If we consider the solution in Table I for which the fraction of $Ca^{2+}$-free dye molecules is the largest ($\mathrm{CaF4}_{eq} \sim 500$ nM, $\mathrm{F4}_{eq} \sim 176$ nM), the correct total weight would be $\sim 0.992/\langle N_{\mathrm{CaF4}}\rangle$ instead of $1/\langle N_{\mathrm{CaF4}}\rangle$ as in Eq. (26). Thus, we expect the ACF that does not include the free dye molecules fluorescence to differ by less than 1% with respect to the one that does.

These theoretical results show that even if only the fluorescence coming from the $Ca^{2+}$-bound dye molecules is collected and that these molecules diffuse with the same coefficient regardless of whether they are free or bound to $Ca^{2+}$, the fact that binding/unbinding reactions between F4 and $Ca^{2+}$ occur within the observation volume makes the corresponding ACF depend on the free diffusion coefficients of $Ca^{2+}$ and E, on their reaction rates, and their concentrations. The aim of the current paper is to analyze under what circumstances some of these biophysical parameters can be derived from the fitting parameters of the ACF. Taking into account that the effective coefficients depend on the concentrations and diffusion coefficients of $Ca^{2+}$, dye, and buffer, by performing experiments for different concentrations it should be possible to identify the coefficients derived from the fittings with those of the theory. Then, combining the estimates obtained under the different conditions, it should be possible to quantify the free diffusion coefficient of $Ca^{2+}$ and its buffer. Moving from theory to practice is not straightforward. To what extent is it possible to quantify all these correlation time scales of the ACF in a real experiment? To what extent the fast reaction approximation provides a good description of what can be measured experimentally? In order to answer these questions we present in what follows the results of FCS experiments performed in solutions together with their analyses within the framework of the theory stated in this section.

TABLE I. Total $Ca^{2+}$ concentrations used in the FCS experiments. All solutions also contained 676 nM $\mathrm{F4}_{tot}$, 9.66 mM $EGTA_{tot}$, 100 mM KCl, 30 mM MOPS and were done at pH 7.2.

| Solution | $\mathrm{Ca}_{tot}$ (mM) |
|---|---|
| A01 | 9.37 |
| A02 | 9.42 |
| A03 | 9.47 |
| A04 | 9.52 |
| A05 | 9.57 |
| A06 | 9.61 |
| A07 | 9.66 |
| A08 | 9.69 |
| A09 | 9.90 |
| A10 | 10.63 |

## III. EXPERIMENTS IN SOLUTION

In this section, we present the results of FCS experiments performed in solutions containing $Ca^{2+}$, the dye, Fluo-4 dextran low affinity, and the $Ca^{2+}$ chelator, EGTA. Fluo-4 is a single-wavelength $Ca^{2+}$ dye that increases its fluorescence about 40 times[63] when bound to $Ca^{2+}$. We list in Table I the set of concentrations for which we performed the experiments. We can observe that they all share the same concentrations of Fluo-4 and EGTA while the $Ca^{2+}$ concentration is varied. All the experiments were performed using an Olympus FluoView 1000 confocal microscope as explained in the Appendix.

### A. Fitting parameters and effective diffusion coefficients

We performed the experiments and fitted the results as explained in the Appendix. Briefly, each (accepted) fluorescence experimental record was divided into ~1021 sub-records of $\sim 2^{13}$ data-points that were subsequently doubled with zeros. The ACFs of each of these sub-records were computed and then averaged. We show in Fig. 2(a) the example of an average ACF (solid curve) with its corresponding fit (dashed curve). Each of these average ACFs were fitted with a two-component model of the form

$$G(\tau) = \sum_{i=0}^{1} \frac{Go_i}{\left(1+\frac{\tau}{\tau_{Di}}\right)\sqrt{1+\frac{\tau}{w^2\tau_{Di}}}}, \tag{27}$$

from which the estimated diffusion coefficients, $D_i$, were computed as $D_i = w_r^2/(4\tau_{Di})$. The experiments were repeated several times using the same solution in the list of Table I and the mean and standard error of the mean of the corresponding estimated weights and diffusion coefficients were then computed for each solution. The diffusion coefficients, $D_0$ and $D_1$, obtained in this way are shown as functions of the total $Ca^{2+}$ concentration in Fig. 2(b) and the corresponding weights, $Go_0$ and $Go_1$, are shown in Fig. 2(c). We also show in Fig. 2(b) the effective coefficients, $D_{ef1}$, $D_{ef2}$, and $D_{ef3}$, and in Fig. 2(c) the weight, $Go_{\mathrm{F4}}$, that we expect to obtain for a system with the concentrations in Table I and the

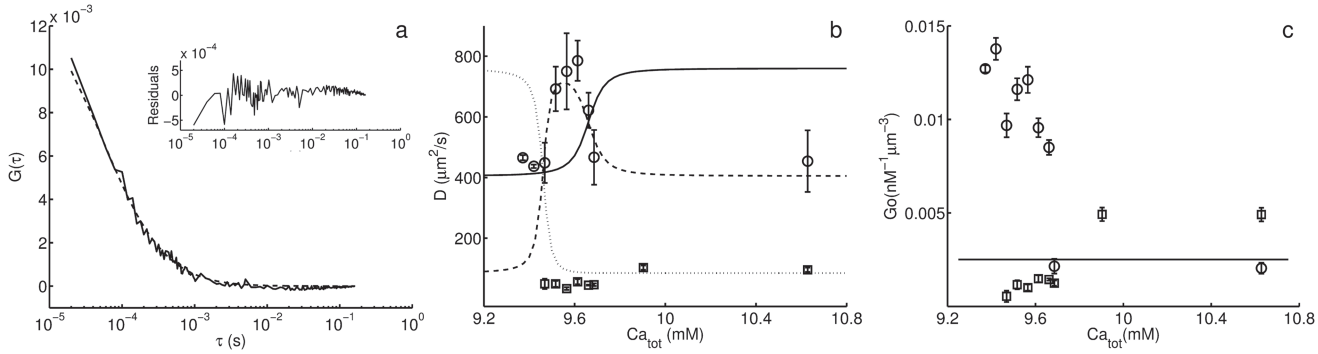


FIG. 2. Experimental ACFs and parameters derived from their fitting. (a) Prototypical example of an (average) ACF obtained in an experiment performed on the solution A03 in Table I (solid curve) and corresponding fit obtained using Eq. (27) (dashed curve). The difference between the two curves is shown in the inset. ((b) and (c)) Parameters derived from the fitting (symbols) and theoretical expected values (curves) as functions of the total $Ca^{2+}$ concentration, $Ca_{tot}$, used to make the solutions: (b) fitted, $D_0$ (squares) and $D_1$ (circles), and effective, $D_{ef1}$ (solid line), $D_{ef2}$ (dotted line), and $D_{ef3}$ (dashed line), diffusion coefficients (the effective coefficients were computed as explained in the Appendix using the parameter values in Tables I and II); (c) fitted, $Go_0$ (squares) and $Go_1$ (circles), and expected, $Go_{F4}$ (solid line), weights. The latter was computed using Eq. (25), the effective volume derived from the calibration, $V_{ef} = 0.59\ \mu m^3$, and the concentrations in Table I.

parameters in Table II. For the computation of $D_{ef1}$, $D_{ef2}$, and $D_{ef3}$, we followed the steps described in the Appendix. These curves differ from those displayed in Fig. 1(d) only in the diffusion coefficient of the buffer, E, which is $D_E = 0$ in Fig. 1(d) and $D_E = 405\mu m^2/s$ in Fig. 2. That is why $D_{ef3}$ goes to zero for large $Ca_{tot}$ in Fig. 1(d) while it approaches $D_E > D_{F4}$ in Fig. 2.

We observe in Fig. 2(b) that the smallest diffusion coefficient that we derive from the fits of the experimental ACFs, $D_0$, remains approximately constant for all the total $Ca^{2+}$ concentrations probed. As illustrated in Fig. 2(c), the weight, $Go_0$, of this component also remains approximately constant. Therefore, we identify $D_0$ with the free diffusion coefficient of Fluo-4 dextran low affinity, $D_{F4}$. The average value over all $Ca^{2+}$ concentrations that we obtain from the fits is $D_0$= (60 ± 7) $\mu m^2/s$, which is compatible with the coefficient obtained from the analysis of solutions of $Ca^{2+}$ and Fluo-4 dextran ((63 ± 6) $\mu m^2/s$).[23] Comparing the other coefficient derived from the fittings, $D_1$, with the expected values, $D_{ef1}$, $D_{ef2}$, and $D_{ef3}$, we see that $D_1 \approx D_{ef1}$ for the experiments with $Ca_{tot} < 9.5$ mM while it is $D_1 \approx D_{ef3}$ for larger concentrations. We also observe that $D_1$ remains approximately constant for the three solutions with the smallest values of $Ca_{tot}$ that we analyzed. Based on the theoretical analysis of Sec. II, we know that the effective coefficients do not change significantly with the reactant concentrations whenever they approach the free diffusion coefficient of some of the reactants. In particular, for $Ca_{tot}$ < 9.5 mM, the expected value of $D_{ef1}$ is approximately equal to the free diffusion coefficient EGTA ($D_E$ = 405 $\mu m^2/s$). Therefore, we assume that $D_1 \approx D_E$ in the experiments with the smallest $Ca_{tot}$ that we probed. We rule out that $D_1$ is approaching $D_{F4}$ because the associated weight, $Go_1$, varies with $Ca_{tot}$. We also rule out that it be approaching $D_{Ca}$ because $D_1$ increases with $Ca_{tot}$ and $D_{Ca}$ is an upper bound for all the free diffusion coefficients of the problem at hand. In this way, the value we estimate for the free diffusion coefficient of EGTA is $D_E = (450 \pm 8)\ \mu m^2/s$.

To give further support to our interpretation of $D_0$ and $D_1$ we show, in Fig. 2(b), the associated weights, $Go_0$ and $Go_1$, derived from the fittings (symbols) and the theoretical weight, $Go_{F4} = 0.0025\ \mu m^{-3}\ nM^{-1}$ (line) calculated using Eq. (25) with the effective volume derived from the calibration, $V_{ef} = 0.59\ \mu m^3$ and the concentrations in Table I. We observe in Fig. 2(b) that $Go_0$ (the weight we associate with $D_{F4}$) remains approximately constant for all $Ca_{tot}$. Its average value over all concentrations is $\langle Go_0 \rangle = (0.0021 \pm 0.0006)\ \mu m^{-3}\ nM^{-1}$. This gives further support to our identification of $D_0$ with $D_{F4}$ given that the theoretical weight of the $D_{F4}$ component ($Go_{F4}$ in Eq. (24)) only depends on the dye concentration (see Eq. (25)) which is the same for all the solutions probed. Inserting the effective volume obtained from the calibration, $V_{ef} = 0.59\ \mu m^3$, and the average, $\langle Go_0 \rangle$, derived from the fittings in Eq. (25) we obtain the estimate $F4_{tot} = (807 \pm 231)$ nM. Taking into account the uncertainties in the final concentrations with which the experiments are performed (see discussion in what follows) and the fact that we are able to fit the ACFs with only two components, this value could be quite different from the theoretical one. It compares reasonably well, however, with the total concentration employed in the construction of the solutions, $F_{tot} = 676$ nM.

TABLE II. Expected values of the various parameters that characterize the system under study.

| Diffusion coefficients and reaction rates | |
|---|---|
| $D_{Ca}$ | 760 $\mu m^2/s$[64] |
| $D_{F4}$ | 85 $\mu m^2/s$[65] |
| $K_{dF4}$ | 2600 nM[a] |
| $k_{off\,F4}$ | 300 $s^{-1}$[66] |
| $D_E$ | 405 $\mu m^2/s$[b] |
| $K_{dE}$ | 150 nM[a] |
| $k_{off\,E}$ | 0.75 $s^{-1}$[66] |

[a]Invitrogen-molecular probes.
[b]Value expected for a 380 *Da* molecule such as EGTA, considering that a 332 *Da* one diffuses with D ~ 425 $\mu m^2/s$ in aqueous solution.[67]

## B. Self-consistency tests

We now perform a set of self-consistency tests of our identification between fitting and biophysical parameters. As

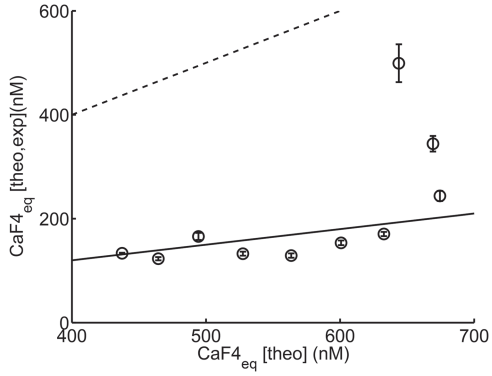


FIG. 3. $Ca^{2+}$-bound dye concentration, $CaF4_{eq}$, estimated using Eq. (26) with the experimental $Go_{tot}$ and $V_{ef} = 0.59\ \mu m^3$ as a function of the theoretically expected $CaF4_{eq}$. The latter was computed assuming a system in equilibrium with $Ca^{2+}$, EGTA, and Fluo-4 using the parameters in Tables I and II. The linear fit of the data points (solid curve) and the identity function (dashed curve) is also shown.

described in Sec. III A, we can estimate the total Fluo-4 concentration, $F4_{tot}$, from the fitting parameter, $Go_0$, and Eq. (25). There is a good agreement between the $F4_{tot}$ estimated from the model and the $F4_{tot}$ concentration employed in the construction of the solution.

$Ca^{2+}$ bound Fluo-4 can be estimated from Eq. (26) setting $Go_{tot} = Go_0 + Go_1$. We show in Fig. 3 the $CaF4_{eq}$ estimated in this way as a function of the theoretical $CaF4_{eq}$ computed using the concentrations in Table I and the dissociation constants $K_{d\mathrm{E}}$ and $K_{d\mathrm{F4}}$ provided by the vendor (Table II). Comparing the linear fit of the experimental points with the identity function (shown in Fig. 3 with solid and dashed curves, respectively), it can be observed that the $Ca^{2+}$-bound dye concentrations derived from the experiments are about one third of the expected ones. We encountered a similar problem when we probed a system with $Ca^{2+}$ and a single wavelength dye[23] and arrived at the conclusion that it could be due to the partial adsorption of reactants in the coverslip. This then means that the actual concentrations in the experiments could be different from those used to prepare the solutions. It is worth noticing that this problem does not affect the effective coefficients since they depend on ratios of the concentrations and the dissociation constant that are not so sensitive to the individual concentration values (at least, within the range explored in our experiments).[23]

We now test whether our identification between the fitted coefficient, $D_1$, and the effective diffusion coefficient, $D_{ef3}$, for $Ca_{tot} > 9.5$ mM is correct. In particular, we analyze if the values that we obtain for $D_{ef3}$ from this identification vary with the concentrations as prescribed by the theory. To this end we recall that, in the experiments, both the buffer, EGTA, and $Ca^{2+}$ are in excess with respect to Fluo-4. Thus, we can assume that the relations Eqs. (20) and (21) that are illustrated in Fig. 1(a) hold in this case. This figure was made using the parameter values that we think characterize the experiments described in this section. Comparing Figs. 1(a) and 2(a) we see that $D_1$ is $D_1 \approx D_{ef3}$ for concentration values for which we expect that $D_{ef3} \approx D_{ef2}^{\mathrm{Ca-E}}$. Therefore, we expect $D_{ef3}$ to depend on the concentrations as prescribed by Eq. (18) with $B = \mathrm{E}$. With this in mind we plotted in Fig. 4(a) the values, $D_1$, obtained for $Ca_{tot} > 9.5$ mM (the ones that we identify with $D_{ef3}$) as a function of the ratio, $\mathrm{E}_{eq}^2/\mathrm{E}_{tot}$, that we computed theoretically using the data in Tables I and II. Fitting the data points of this figure with the function

$$f(x) = (\alpha + \beta x)/(1 + \gamma x) \tag{28}$$

and identifying $\alpha = D_{\mathrm{E}}$, $\beta = D_{\mathrm{Ca}}/K_{d\mathrm{E}}$ and $\gamma = 1/K_{d\mathrm{E}}$, in principle, we could derive estimates of the free diffusion coefficients of EGTA and $Ca^{2+}$ and the dissociation constant of their reaction that can be compared with their expected values. Eq. (28) fits reasonably well the experimental data (solid curve in Fig. 4(a)), obtaining $\alpha = (429 \pm 80)\ \mu m^2/s$, $\beta = (5.06 \pm 5.05)\ \mu m^2\ s^{-1}\ nM^{-1}$, and $\gamma = (0.0065 \pm 0.0069)\ nM^{-1}$. This leads to $D_{\mathrm{E}} = (429 \pm 80)\ \mu m^2/s$ which compares very well with the expected value ($\sim$405 $\mu m^2/s$). The uncertainties in the values of $\beta$ and $\gamma$, however, are too large to derive a meaningful estimate of $K_{d\mathrm{E}}$ from $\gamma$ and, therefore, of $D_{\mathrm{Ca}}$ combining $\beta$ and $\gamma$. In spite of these large uncertainties, the mean value $\gamma = 0.0065\ nM^{-1}$ gives $K_{d\mathrm{E}} \sim 153$ nM which is almost equal to the value prescribed by the vendor ($K_{d\mathrm{E}} \sim 150$ nM). If we use $\beta = 5\ \mu m^2\ s^{-1}\ nM^{-1}$ and $K_{d\mathrm{E}} = 153$ nM we obtain $D_{\mathrm{Ca}} = 765\ \mu m^2/s$ which is also very close to the free diffusion coefficient of $Ca^{2+}$ in aqueous solutions.

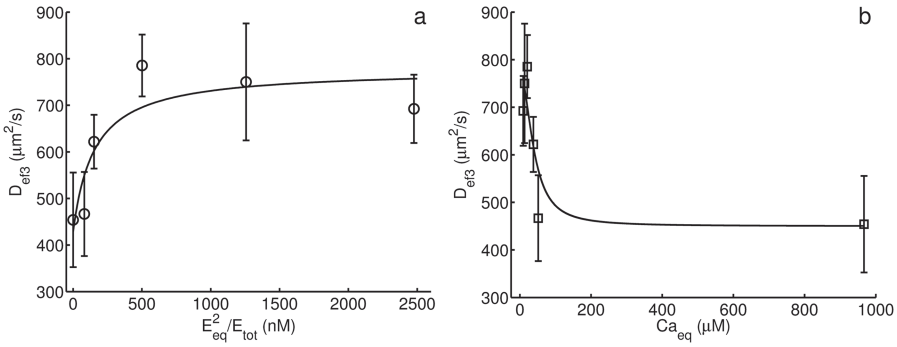


FIG. 4. Effective diffusion coefficients, $D_{ef3}$, obtained under the assumption that they are given by the fitted values, $D_1$, derived from the experiments with $Ca_{tot} > 9.5$ mM. (a) $D_{ef3}$ as functions of $\mathrm{E}_{eq}^2/\mathrm{E}_{tot}$. We fit the displayed data points (circles) with a curve of the form Eq. (28) (solid line). (b) $D_{ef3}$ as functions of $Ca_{eq}$, the data (squares) were fitted with a curve of the form Eq. (29) (solid line). The ratios, $\mathrm{E}_{eq}^2/\mathrm{E}_{tot}$, and the values of $Ca_{eq}$ were computed theoretically assuming a system in equilibrium with $Ca^{2+}$, EGTA, and Fluo-4 using the parameters in Tables I and II.

Thus, in spite of the large uncertainties with which $\beta$ and $\gamma$ can be derived by fitting the data, the figure provides an indication that the ratio $D_{ef3}/D_{\rm ca}$ depends on $E_{eq}^2/E_{tot}$ as expected based on our theory and assumptions. This gives further support to our interpretation of the information that is carried by the fitted coefficient, $D_1$.

We must recall that, according to Eq. (24), the component of the ACF associated with $D_{ef3}$ also has an exponentially decaying term, $\exp(-\nu_3\tau)$, that we could not derive from the fitting. This could be due to the fact that $\exp(-\nu_3\tau) \approx 1$ for $\tau \sim \tau_{ef3} = w_r^2/(4D_{ef3})$. In fact the expected values of $\exp(-\nu_3\tau_{ef3})$ are larger than 0.99 for all solutions with the exception of the one labelled A10 for which it is 0.81. The expected value, $\nu_3$, for this last solution is ~5 ms$^{-1}$ while it is within 0.38–1.25 ms$^{-1}$ for the others. The expected values of $\tau_{ef3}$, on the other hand, lie within the range 0.015–0.044 ms.

### C. Estimation of the $Ca^{2+}$ free diffusion coefficient and the buffering parameters

One of the main goals of the present paper is to test whether FCS experiments performed with single-wavelength $Ca^{2+}$ dyes can be used to derive the parameters that characterize the $Ca^{2+}$ traps that compete with the dye even though they are non-fluorescent. With this in mind, we now analyze the experiments as if we did not have any *a priori* information on the trap (EGTA in our experiments) in order to test if what we can deduce from such a "blind" analysis agrees with what we know. We assume that only the total Fluo-4 concentration is known. We first focus on $D_1$. As already mentioned in connection with Fig. 2, we have associated the decreasing values of $D_1$ with $D_{ef3} \approx D_{ef2}^{\rm Ca-E}$ given by Eq. (18) with $B$ = E. We rewrite this equation in terms of $Ca^{2+}$ as

$$D_{ef2}^{\rm Ca-E} = \frac{K_{d\rm E}E_{tot}D_{\rm Ca} + (Ca_{eq} + K_{d\rm E})^2 D_{\rm E}}{K_{d\rm E}E_{tot} + (Ca_{eq} + K_{d\rm E})^2}. \quad (29)$$

Given that $E_{tot}$ is the same for all the experiments, Eq. (29) implies that, if the number of different solutions probed is large enough, knowing the free concentration, $Ca_{eq}$, for each solution and using $D_1 \approx D_{ef2}^{\rm Ca-E}$, the values, $K_{d\rm E}$, $D_{\rm E}$, $E_{tot}$, and $D_{\rm Ca}$ could, in principle, be inferred. In order to estimate the free $Ca^{2+}$ concentration for each solution, we can proceed as follows: use the weights, $Go_{tot}$ and $Go_{\rm F4}$, to compute $CaF4_{eq}$ = $1/(V_{ef}Go_{tot})$ and $F4_{tot} = 1/(V_{ef}Go_{\rm F4})$ and, from them, determine $F4_{eq} = F4_{tot} - CaF4_{eq}$. Using the dissociation constant, $K_{d\rm F4}$, provided by the vendor we can then estimate the free $Ca^{2+}$ concentration in each solution as

$$Ca_{eq} = \frac{K_{d\rm F4}CaF4_{eq}}{F4_{eq}} = K_{d\rm F4}\frac{Go_{\rm F4}}{(Go_{tot} - Go_{\rm F4})}. \quad (30)$$

This computation, however, makes extensive use of the weights which we argued could have been inferred with relatively large uncertainties in the example at hand. In order to ponder whether we can proceed as described, as a first step we plot the fitted coefficients, $D_1$, that correspond to the solutions A4-A8 and A10 (which we identify with $D_{ef2}^{\rm Ca-E}$, $D_1$ = 692 $\mu$m$^2$/s, 750 $\mu$m$^2$/s, 785 $\mu$m$^2$/s, 622 $\mu$m$^2$/s, 467 $\mu$m$^2$/s, and 454 $\mu$m$^2$/s) as functions of the free theoretical $Ca^{2+}$ concentration (i.e., the one that is derived from the concentrations used to make the solutions). This is shown with squares in Fig. 4(b). We then fit them using a simplified version of Eq. (29) in which we replaced $(Ca_{eq} + K_{d\rm E})^2$ by $(Ca_{eq})^2$ (the very large difference between $Ca_{eq}$ and $K_{d\rm E}$ makes it impossible to extract a reliable value of $K_{d\rm E}$ separately),

$$D_{ef2}^{\rm Ca-E} = \frac{K_{d\rm E}E_{tot}D_{\rm Ca} + Ca_{eq}^2 D_{\rm E}}{K_{d\rm E}E_{tot} + Ca_{eq}^2}. \quad (31)$$

The result of the fitting is shown in Fig. 4(b) with a solid curve. From the fit we obtain $D_{\rm Ca}$ = (772 ± 98) $\mu$m$^2$/s and $K_{d\rm E}E_{tot}$ = (1550 ± 1747) $\mu$M$^2$. The diffusion coefficient is within the expected value and the value derived otherwise in this paper. In the case of $K_{d\rm E}E_{tot}$, we observe that although the fitted mean, 1550 $\mu$M$^2$, is relatively close to the theoretical value, ~1500 $\mu$M$^2$, the uncertainty with which it is determined is extremely large. These preliminary computations indicate that the diffusion coefficients, $D_1$ and $D_2$, that are derived by fitting the ACF change with the various concentrations as predicted by the theory. However, even if it is possible to derive from them reliable values of the free diffusion coefficients, the concentrations or dissociation constants that can be inferred usually carry huge uncertainties. We now analyze what happens if we work "blindly" as described previously, i.e., if we compute the free $Ca^{2+}$ concentration for each solution using Eq. (30). When trying to do so, the problem we face for the experimental conditions that we probe in this paper is that, by construction, the fraction $F4_{tot}/CaF4_{eq}$ is very close to unity (it varies between 1.008 and 1.53). Given Eqs. (25) and (26), this implies that the difference $Go_{tot}/Go_{\rm F4} - 1$ varies between 0.008 and 0.53. Thus, any error in the estimates of $Go_{tot}$ or $Go_{\rm F4}$ is greatly amplified by the use of Eq. (30) leading to poor estimates of $Ca^{2+}$. In fact, if we use Eq. (30) we obtain, for the various solutions, the concentration values, $Ca_{eq}$ = 260 nM, 457 nM, 403 nM, 440 nM, 1507 nM, 6258 nM, which are between 18 and 150 times smaller than those that can be computed using the construction conditions. In spite of this huge discrepancy in the concentration values, we did insert them "blindly" in Eq. (31) together with the estimate, $D_{\rm E} \approx D_1$, derived from the data points of Fig. 2 in the region where $D_1$ does not vary significantly ($D_{\rm E}$ = (450 ± 8) $\mu$m$^2$/s) and the six values of $D_1$ that we identify with $D_{ef2}^{\rm Ca-E}$ as before. Fitting Eq. (29) with this information, we obtained $D_{\rm Ca}$ = (774 ± 157) $\mu$m$^2$/s and $K_{d\rm E}E_{tot}$ = (0.42 ± 0.82) $\mu$M$^2$. In this case, the estimated value of $K_{d\rm E}E_{tot}$ is much smaller than expected because of the poor $Ca_{eq}$ estimates but the inferred free diffusion coefficient of $Ca^{2+}$, strikingly, is still very close to the known one.

## IV. DISCUSSION AND CONCLUSIONS

In this paper, we have presented the results of FCS experiments performed in a medium with $Ca^{2+}$, a single wavelength $Ca^{2+}$ dye (Fluo-4), and a $Ca^{2+}$ trap (EGTA) together with the theory to analyze them and derive quantitative information on diffusion coefficients and $Ca^{2+}$ trapping parameters. We first analyzed the diffusive time scales that characterize the dynamics of a system with these three species (Eqs. (3)–(7)). Although their expressions are quite complicated, under certain conditions they can be approximated by the effective

coefficients of the systems with $Ca^{2+}$ and one of the other two species (see Fig. 1). These approximated expressions were particularly useful for the analysis of the experiments. After having studied the time scales that characterize the reaction-diffusion system, we derived an analytic expression of the Auto-Correlation Function (ACF) of the fluorescence fluctuations under the assumption that the reaction time scale was fast enough.[22] The resulting ACF, Eq. (24), had 4 components, one of them exact and associated with the free diffusion coefficient of the dye. The other three were characterized by the effective coefficients of the three species reaction-diffusion system. Two of the latter had exponentially decaying terms as well. We then presented the results of a set of experiments performed in solutions containing the same total EGTA and dye concentrations but different total $Ca^{2+}$ concentrations as listed in Table I. The dye used was Fluo-4 low affinity. Even though the theory predicts that the ACF has 4 components and six time scales, it is not always possible to derive reliable values of so many fitting parameters. For this reason, we tried several expressions with 1, 2, or 3 components and with and without exponential factors. Based on a $\chi^2$ comparison of the difference between the fitted and the experimental ACF, we concluded that the fits with two purely diffusive components were the best. Comparing the two weights, $Go_0$ and $Go_1$, and diffusion coefficients, $D_0$ and $D_1$, derived from the fitting of each set of experiments in Table I, we observed that $D_0$ and $Go_0$ remained constant for all sets (see Fig. 2). We then identified $D_0$ with the free diffusion coefficient of the dye, $D_{\mathrm{F4}}$. Averaging over all experiments and computing the standard deviation, we obtained $D_{\mathrm{F4}} = (60 \pm 7)$ $\mu m^2/s$. This value is similar to the coefficient obtained from the analysis of solutions of $Ca^{2+}$ and Fluo-4 dextran, $D_{\mathrm{F4}} = (63 \pm 6)$ $\mu m^2/s$.[23] Comparing the behavior of the other coefficient derived from the fittings, $D_1$, with that of the effective coefficients prescribed by the theory computed with the expected concentration and free coefficient values (Fig. 2) allowed us to infer how it depended on the biophysical parameters of the system. Identifying $D_1$ with the effective coefficient $D_{ef1}$ and considering that for low $Ca^{2+}$ concentrations, $D_{ef1} \sim D_E$, for the smallest $Ca^{2+}$ concentrations probed, we could estimate the free diffusion coefficient of EGTA. We obtained $D_{\mathrm{E}} = (450 \pm 8)$ $\mu m^2/s$ which is close to the value we can expect ($D \sim 405$ $\mu m^2/s$) for a 380 *Da* molecule such as EGTA, considering that a 332 *Da* one diffuses at D ~ 425 $\mu m^2/s$ in solution.[67]

Using information on the weights, we could estimate the concentrations of free and $Ca^{2+}$-bound dye for each solution. The average value of $F4_{tot}$ gave (807 ± 231) nM, which is consistent with the total concentration employed in the construction of the solutions, $F_{tot} = 676$ nM. The values of $CaF4_{eq}$ differed by a factor of 3 with respect to those that corresponded to the concentrations that we used to construct the solutions (see Fig. 3). Using the estimated values of $F4_{eq}$ and $CaF4_{eq}$ and the dissociation constant, $K_{d\mathrm{F4}}$, provided by the vendor, we could, in principle, derive the concentration of free $Ca^{2+}$ for each solution using Eq. (30). The conditions of the experimental solutions, however, were such that the denominator in Eq. (30) was very small which led to large uncertainties in the estimated concentrations. In any case, inserting these concentrations (that were quite different from the expected ones) into Eq. (31) gave a correct estimate of the free diffusion coefficient of $Ca^{2+}$, $D_{\mathrm{Ca}} = (774 \pm 157)$ $\mu m^2/s$. The obtained mean value of $K_{d\mathrm{E}}\,\mathrm{E}_{tot}$, however, was very poor and with a large uncertainty. We do not expect to encounter such a problem when applying the approach introduced here to experiments performed in intact cells under basal conditions. Namely, in such a case free $Ca^{2+}$ is of the order of 100 nM so that the difference $CaF_{eq}/F4_{tot} - 1$ can be safely bounded away from 1 thus preventing the denominator in Eq. (30) from becoming too small. Furthermore, the adsorption of the reactants by the coverslip that might be affecting the experiments in solution would not be present in that either. We also analyzed the dependence with the theoretical free $Ca^{2+}$ concentrations of the values, $D_1$, that we identified with $D_{ef2}^{Ca-E}$. The data points shown in Fig. 2(b) could be fitted with Eq. (31). We used this simplified version of Eq. (29) because $Ca_{eq} \ll K_{d\mathrm{E}}$ for the conditions of the experiments and it was impossible to obtain a reliable estimate of $K_{d\mathrm{E}}$ separately. We expect this situation to be different in intact cells as well. Namely, in the cytosol we expect the dissociation constant of endogenous $Ca^{2+}$ buffers to be larger or comparable to the basal cytosolic concentration, $Ca_{eq} \sim 100$ nM. Thus, in principle it should be possible to estimate both $K_{d\mathrm{E}}$ and $K_{d\mathrm{E}}\,\mathrm{E}_{tot}$. In the experiments analyzed here, the values derived from this fitting yielded $D_{\mathrm{Ca}} = (772 \pm 98)$ $\mu m^2/s$ and $K_{d\mathrm{E}}\,\mathrm{E}_{tot} = (1550 \pm 1747)$ $\mu M^2$. The $Ca^{2+}$ free diffusion coefficient was again within its expected value with a reasonable uncertainty. Although the mean of $K_{d\mathrm{E}}\,\mathrm{E}_{tot}$ improved with respect to the one estimated using the values, $Ca_{eq}$, derived from the experiments, its uncertainty was still too large. We thus conclude that there are two separate problems affecting the estimates that can be obtained from the non-fluorescent $Ca^{2+}$ buffer concentration and its dissociation constant using only the FCS experiment data. On the one hand, obtaining reliable estimates of the weights of the FCS requires that very long experiments be performed.[34] Then, there is the additional problem that arises if the individual weights are very different between themselves. For the solutions probed in the present paper, the weight of the term that corresponded to the free diffusion of the dye was very small compared to the total weight in many cases. That introduces an additional source of variability because any uncertainty in the larger weight translates into a large error in the smaller one. This situation can be improved by choosing adequate dye concentrations depending on the system to be probed. But beyond the errors of the individual weights, fitting functions like the one in Eq. (29) requires to have enough experimental data points in a particular region of free $Ca^{2+}$ concentrations so that its fitting parameters can be inferred with a reasonable uncertainty. In any case, even with large uncertainties, what we have observed in our experiments in solution is that the derived mean value of $K_{d\mathrm{E}}\,\mathrm{E}_{tot}$ was fairly close to the expected ones if we used the theoretical free $Ca^{2+}$ concentration values. This shows that the analysis of FCS experiments performed under various conditions using single wavelength $Ca^{2+}$ dyes can provide information on the properties of the non-fluorescent buffers with which $Ca^{2+}$ interacts (in this case, EGTA), buffers that compete with the dye for the ions. This opens the possibility of applying a similar approach to study $Ca^{2+}$ diffusion and $Ca^{2+}$ buffering in intact cells. In such a case, several buffers are

competing for $Ca^{2+}$. Thus, the problem is much more complicated than the experiments that we have done and analyzed in this paper. We expect however that a similar analysis would provide information on some sort of "effective buffer," particularly, on the cell buffering capacity. It would also allow us to quantify the free diffusion coefficient of $Ca^{2+}$ in the cytosol, a parameter that was estimated over 20 years ago in cytosolic extracts[10] but not in intact cells. The actual meaning of the "free diffusion coefficients" that could be derived from such FCS experiments should be interpreted within the context that displacement in cells is spatially restricted.[68] The free transport rates that could be inferred would then be limited by the time resolution with which the data are acquired so that they would not necessarily correspond to the rates that rule diffusion at the shortest possible length scales.[69–71] In order to replicate in intact cells the type of approach that we have presented in this paper, we would need to perform FCS experiments under different conditions. Given the restrictions on the low concentrations of dye that should be used, almost the only choice that we are left with is to change the basal $Ca^{2+}$ concentration. Preliminary tests performed in *Xenopus laevis* oocytes using caged $Ca^{2+}$ that is continuously photoreleased to keep a constant concentration show that this is an option. We thus expect to be able to present soon the results on the quantification of $Ca^{2+}$ diffusion and buffering in these cells following the approach introduced in this paper.

## ACKNOWLEDGMENTS

This research has been supported by UBA (Grant No. UBACyT 20020130100480BA) and ANPCyT (Grant No. PICT 2013-1301). L.S. and S.P.D. are members of Carrera del Investigador Científico (CONICET).

## APPENDIX: MATERIALS AND METHODS

### 1. Theory: Computation of effective diffusion coefficients for a system with $Ca^{2+}$, dye, and chelator

As explained in the main body of the paper, the linearization of the reaction-diffusion system, Eqs. (3)–(7), around the equilibrium solution is characterized by 5 branches of eigenvalues, one of them associated with the free diffusion coefficient of the dye, Fluo-4 and another to that of EGTA. The third eigenvalue, when expanded up to $\mathcal{O}(q^2)$, in the wavenumber, $q$, corresponds to the effective diffusion coefficient, $D_{ef\,1}$, given by Eq. (14). The expansion of the remaining two eigenvalues up to $\mathcal{O}(q^2)$ also has a diffusive component with coefficients, $D_{ef\,2}$ and $D_{ef\,3}$, as shown in Eqs. (12)–(13). Using algebraic manipulation software it is possible to obtain analytic expressions for $D_{ef\,2}$ and $D_{ef\,3}$. We did not include them in the main body of the paper because they are too long. Here we describe briefly the steps that yield all the effective coefficients. In Fourier space, the branches of eigenvalues of the matrix that rules the dynamics of the linear version of Eqs. (3)–(7) are

$$\lambda_1 = -D_{\rm F}\, q^2, \tag{A1}$$

$$\lambda_2 = -D_{\rm E} q^2, \tag{A2}$$

$$\lambda_3 = -\frac{\Sigma}{3} + \frac{2^{-1/3}}{3}\left(m + \sqrt{m^2 + 4(-\Sigma^2 + 3u)^3}\right)^{1/3} - \frac{1}{3}\frac{2^{1/3}(-\Sigma^2 + 3u)}{\left(m + \sqrt{m^2 + 4(-\Sigma^2 + 3u)^3}\right)^{1/3}}, \tag{A3}$$

$$\lambda_4 = -\frac{\Sigma}{3} - \frac{1}{6}(1 - i\sqrt{3})2^{-1/3}\left(m + \sqrt{m^2 + 4(-\Sigma^2 + 3u)^3}\right)^{1/3} + \frac{1}{6}\frac{(1 + i\sqrt{3})2^{1/3}(-\Sigma^2 + 3u)}{\left(m + \sqrt{m^2 + 4(-\Sigma^2 + 3u)^3}\right)^{1/3}}, \tag{A4}$$

$$\lambda_5 = \bar{\lambda_4}, \tag{A5}$$

where $i$ is the imaginary unit and

$$\Sigma = a + a_{\rm E} + 1 + c + c_{\rm E} + k_{\rm E} + q^2\,(1 + D_{\rm F4} + D_{\rm E}),$$

$$u = q^4(D_{\rm E} + D_{\rm F4} + D_{\rm E}D_{\rm F4}) + q^2[(D_{\rm F4} + 1)(c_{\rm E} + k_{\rm E}) + (D_{\rm E} + 1)(1 + c) + (D_{\rm F4} + D_{\rm E})(a + a_{\rm E})] + a(c_{\rm E} + k_{\rm E}) + (1 + c)(a_{\rm E} + c_{\rm E} + k_{\rm E}),$$

$$m = a_1 + b_1 q^2 + c_1 q^4 + d_1 q^6,$$

$$a_1 = -2\,(1 + a + c)^3 - 2\,k_{\rm E}(1 + a + c_{\rm E})^3 + 3\,k_{\rm E}(1 + a_{\rm E} + c_{\rm E}) \times (1 + a + c)^2 + 3\,k_{\rm E}^2(1 + a + c)(1 + a_{\rm E} + c_{\rm E})^2 - 9\,a\,a_{\rm E}\,k_{\rm E}\,[(1 + a + c) + k_{\rm E}(1 + a_{\rm E} + c_{\rm E})],$$

where $a = \frac{\mathrm{F4}_{tot}}{K_{d\mathrm{F4}}}$, $a\mathrm{E} = \frac{\mathrm{E}_{eq}}{K_{d\mathrm{E}}}\,k_{\rm E}$, $c = \frac{\mathrm{Ca}_{eq}}{K_{d\mathrm{F4}}}$, and $cE = \frac{\mathrm{Ca}_{eq}}{K_{\rm E}}\,k_{\rm E}$. In spite of the complex notation, it can be shown that the eigenvalues are real functions of $q^2$. We do not include the expressions of $b_1$, $c_1$, and $d_1$ because they do not enter the effective coefficients. Expanding the eigenvalues, $\lambda_3$, $\lambda_4$, and $\lambda_5$ up to $\mathcal{O}(q^2)$ and using the identification introduced in Eqs. (11)–(13) we arrive at Eq. (14) for $D_{ef\,1}$. In order to compute numerically the values, $\nu_{ef\,2}$ and $\nu_{ef\,3}$, we set $q^2 = 0$ in the expansions of $\lambda_4$ and $\lambda_5$. In order to determine $D_{ef\,2}$ and $D_{ef\,3}$ numerically, we calculate the differences, $\lambda_4 - \nu_{ef\,2}$ and $\lambda_5 - \nu_{ef\,3}$, using the expansions of the eigenvalues up to $\mathcal{O}(q^2)$ and then set $q = 1$.

### 2. Experiments: Data acquisition

The FCS experiments were done depositing on a coverslip a 30 $\mu$l drop of the chosen solution. The fluorescence records were obtained in a FV1000 spectral confocal microscope using a 60× oil immersion objective (UPlasSapo), NA 1.35, a 115 $\mu$m pinhole size, illuminating the sample with the 488 nm line of an argon laser and collecting the emitted light in the 500–600 nm range. The fluorescence was collected from a single point located at approximately 20 $\mu$m from the coverslip at a 50 kHz acquisition rate during ~160 $s$. We performed series of experiments at various laser powers to determine the optimal power range that prevented photobleaching and yet provided good correlations (data not shown).

### 3. Computation of the experimental ACF

The ACF was computed after having verified that the fluorescence fluctuated about a steady value during the time course of the experiment. Records that presented abrupt changes were discarded. The fluorescence time series was divided into N segments of length, FTL, each of which was doubled by adding FTL zeros in order to avoid aliasing. A discrete Fourier transform was applied to each segment and the ACF was then computed using the Wiener-Khinchin theorem. The N ACFs were then averaged. FTL sets a limit on the longest correlation time that can be derived from the ACF. Thus, for these experiments we used FTL = $2^{13}$ which gave N = 1021, 164 ms segments. The longest correlation time that we could identify was 1 ms. The first 1-2 points of the ACF were discarded in order to avoid the effects of after-pulsing.

### 4. Fitting the experimental ACF

The averaged ACFs were fitted using functions of the general form

$$G(\tau) = \sum_{i=0}^{m} Go_i \frac{e^{-\nu_i \tau}}{\left(1 + \frac{\tau}{\tau_{D_i}}\right)\sqrt{1 + \frac{\tau}{w^2 \tau_{D_i}}}} \tag{A6}$$

with different numbers of components with either $\nu_i$ as a fitting parameter or with $\nu_i = 0$. The best fits were obtained using $m = 2$ and $\nu_0 = \nu_1 = 0$. The analysis presented in Sec. III involves analyzing how to establish the way in which the fitted parameters of the experiments are related to those of the theoretical ACF (Eq. (24)). For the fittings we used the function nlinfit that comes with Matlab.[72] In order to apply this method, it is necessary to give an initial guess of the fitting parameters. We tried several initial guesses and discarded those that gave diffusion coefficients, $D$, and weights, $Go$, that were outside these ranges: 10 $\mu$m$^2$/s < $D$ < 2500 $\mu$m$^2$/s and 0 < $Go$ < 10. When the optimization algorithm gave more than one set of fitting parameters, we chose the one that gave the smallest $\chi^2$ given by

$$\chi^2 = \frac{1}{N_p - N_v} \sum_{i}^{N_p} \frac{(G_{theo}(\tau_i) - G_{exp}(\tau_i))^2}{G_{theo}(\tau_i)} \tag{A7}$$

with $N_p$ the total number of data points of the experimental ACF, $G_{exp}$, $N_v$ the number of variables of the model $G_{theo}$ the ACF computed with the fitting model. In order to go from the diffusive correlation times to the diffusion coefficients, we calibrated the confocal volume using a solution containing 50 nM of fluorescein whose diffusion coefficient was assumed to be 425 $\mu$m$^2$/s.[67,73] The resulting values of the lateral width, $w_r$, varied between 262 and 291 nm with $w = w_z/w^r = 5$ and the estimated effective volume was $V_{ef}$ = (0.59 ± 0.1) $\mu$m$^3$. Had we used 300 $\mu$m$^2$/s for the diffusion coefficient of fluorescein as done in Ref. 32 we would have obtained $V_{ef}$ = 0.35$\mu$m$^3$ and diffusion coefficients that differed by a factor ~0.7 from those presented in the paper.

### 5. Parameter estimation and error propagation

Parameters obtained by fitting the experimental ACF, diffusion coefficients, $D$, and weights, $Go$, were expressed as the mean ± standard error of the mean (SEM). Other results were expressed as the value ± the uncertainty obtained from the error propagation.


[1] M. J. Berridge, M. D. Bootman, and P. Lipp, Nature **395**, 645 (1998).
[2] M. D. Bootman, Cold Spring Harbor Perspect. Biol. **4**, a011171 (2012).
[3] M. T. Nelson, H. Cheng, M. Rubart, L. F. Santana, A. D. Bonev, H. J. Knot, and W. J. Lederer, Science **270**, 633 (1995).
[4] M. Nishiyama, K. Hong, K. Mikoshiba, M.-m. Poo, and K. Kato, Nature **408**, 584 (2000).
[5] G. Dupont, S. Swillens, C. Clair, T. Tordjmann, and L. Combettes, Biochim. Biophys. Acta, Mol. Cell Res. **1498**, 134 (2000).
[6] D. P. Noren, W. H. Chou, S. H. Lee, A. A. Qutub, A. Warmflash, D. S. Wagner, A. S. Popel, and A. Levchenko, Sci. Signaling **9**, ra20 (2016).
[7] B. Zhivotovsky and S. Orrenius, "Special issue on $Ca^{2+}$ signaling mechanisms of cell survival and cell death," Cell Calcium **50**, 211 (2011).
[8] X.-P. Sun, N. Callamaras, J. S. Marchant, and I. Parker, J Physiol. **509**, 67 (1998).
[9] A. P. Thomas, G. S. Bird, G. Hajnòczky, L. D. Robb-Gaspers, and J. W. Putney, FASEB J. **10**, 1505 (1996).
[10] N. Allbritton, T. Meyer, and L. Stryer, Science **258**, 1812–1815 (1992).
[11] B. Schwaller, Cold Spring Harbor Perspect. Biol. **2**, a004051 (2010).
[12] A. Biess, E. Korkotian, and D. Holcman, PLoS Comput. Biol. **7**, 1 (2011).
[13] P. C. Bressloff and J. M. Newby, Rev. Mod. Phys. **85**, 135 (2013).
[14] S. L. Dargan and I. Parker, J. Physiol. **553**, 775 (2003).
[15] S. L. Dargan, B. Schwaller, and I. Parker, J. Physiol. **556**, 447 (2004).
[16] B. Pando, S. P. Dawson, D.-O. D. Mak, and J. E. Pearson, Proc. Natl. Acad. Sci. U. S. A. **103**, 5338 (2006).
[17] A. Einstein, *The Collected Papers of Albert Einstein, Volume 2, Translated by Anna Beck, Consultant Peter Havas* (Princeton University Press, Princeton, 1989).
[18] A. Einstein, *Investigations on the Theory of the Brownian Movement* (Courier Dover Publications, 1956).
[19] L. Sigaut, J. E. Pearson, A. Colman-Lerner, and S. Ponce Dawson, PLoS Comput. Biol. **10**, e1003629 (2014).
[20] B. Sprague, R. Pego, D. Stavreva, and J. McNally, Biophys. J. **86**, 3473 (2004).
[21] L. Sigaut, M. L. Ponce, A. Colman-Lerner, and S. P. Dawson, Phys. Rev. E **82**, 051912 (2010).
[22] E. P. Ipiña and S. P. Dawson, Phys. Rev. E **87**, 022706 (2013).
[23] L. Sigaut, C. Villarruel, M. L. Ponce, and S. P. Dawson, e-print arXiv:1608.00064v1 (2016).
[24] D. Magde, E. Elson, and W. W. Webb, Phys. Rev. Lett. **29**, 705 (1972).
[25] K. Berland, P. So, and E. E. Gratton, Biophys. J. **68**, 694701 (1995).
[26] P. Schwille, U. Haupts, S. Maiti, and W. W. W, Biophys. J. **77**, 2251 (1999).
[27] E. L. Elson, Traffic **2**, 789 (2001).
[28] S. A. Kim and P. Schwille, Curr. Opin. Neurobiol. **13**, 583 (2003).
[29] D. Grünwald, M. C. Cardoso, H. Leonhardt, and V. Buschmann, Curr. Pharm. Biotechnol. **6**, 381 (2005).
[30] D. C. Lamb, A. Schenk, C. Röcker, C. Scalfi-Happ, and G. Ulrich Nienhaus, Biophys. J. **79**, 1129 (2000).
[31] E. Bismuto, E. Gratton, and D. C. Lamb, Biophys. J. **81**, 3510 (2001).
[32] M. A. Digman, P. Sengupta, P. W. Wiseman, C. M. Brown, A. R. Horwitz, and E. Gratton, Biophys. J. **88**, L33L36 (2005).
[33] E. Haustein and P. Schwille, Annu. Rev. Biophys. Biomol. Struct. **36**, 151 (2007).
[34] E. P. Ipiña and S. P. Dawson, Biophys. J. **107**, 2674 (2014).
[35] J. R. Lakowicz, *Principles of Fluorescence Correlation Spectroscopy* (Springer, USA, 2007).
[36] E. Elson, Biophys. J. **101**, 2855 (2011).
[37] N. L. Thompson, P. Navaratnarajah, and X. Wang, J. Phys. Chem. B **115**, 120 (2011).
[38] J. Mütze, T. Ohrt, and P. Schwille, Laser Photonics Rev. **5**, 52 (2011).
[39] N. Petersen, P. Höddelius, P. Wiseman, O. Seger, and K. Magnusson, Biophys. J. **65**, 1135 (1993).
[40] C. M. Brown, R. B. Dalal, B. Hebert, M. A. Digman, A. R. Horwitz, and E. Gratton, J. Microsc. **229**, 78 (2008).
[41] B. Hebert, S. Costantino, and P. W. Wiseman, Biophys. J. **88**, 3601 (2005).
[42] M. Eigen and R. Rigler, Proc. Natl. Acad. Sci. U. S. A. **91**, 5740 (1994).
[43] P. Schwille, F. Meyer-Almes, and R. Rigler, Biophys. J. **72**, 1878 (1997).

[44]L. Estrada, M. Roberti, S. Simoncelli, V. Levi, P. Aramendía, and O. Martínez, J. Phys. Chem. B **116**, 2306 (2012).
[45]G. Kaur, M. W. Costa, C. M. Nefzger, J. Silva, J. C. Fierro-Gonzalez, J. M. Polo, D. M. Bell, and N. Plachta, Nat. Commun. **4**, 1637 (2012).
[46]M. D. White, J. F. Angiolini, Y. D. Alvarez, G. Kaur, Z. W. Zhao, E. Mocskos, L. Bruno, S. Bissiere, V. Levi, and N. Plachta, Cell **165**, 75 (2016).
[47]M. Wachsmuth, C. Conrad, J. Bulkescher, B. Koch, R. Mahen, M. Isokane, R. Pepperkok, and J. Ellenberg, Nat. Biotechnol. **33**, 384 (2015).
[48]C. Di Rienzo, E. Gratton, F. Beltram, and F. Cardarelli, Proc. Natl. Acad. Sci. U. S. A. **110**, 12307 (2013).
[49]A. Diaspro, F. Federici, and M. Robello, Appl. Opt. **41**, 685 (2002).
[50]J. Enderlein, I. Gregor, D. Patra, and J. Fitter, Curr. Pharm. Biotechnol. **5**, 155 (2004).
[51]J. Enderlein, I. Gregor, D. Patra, T. Dertinger, and U. B. Kaupp, Chem. Phys. Chem. **6**, 2324 (2005).
[52]C. Pieper, K. Wei, I. Gregor, and J. Enderlein, in *Methods in Enzymology*, Vol. 518 Fluorescence Fluctuation Spectroscopy (FFS), Part A, edited by S. Y. Tetin (Academic Press, 2013), pp. 175–204.
[53]R. M. Paredes, J. C. Etzler, L. T. Watts, W. Zheng, and J. D. Lechleiter, Methods **46**, 143 (2008).
[54]C. DiRienzo, E. Gratton, F. Beltram, and F. Cardarelli, Biophys. J. **111**, 679 (2016).
[55]J. Enderlein, Phys. Rev. Lett. **108**, 108101 (2012).
[56]R. Shusterman, T. Gavrinyov, and O. Krichevsky, Phys. Rev. Lett. **100**, 098102 (2008).
[57]C. DiRienzo, F. Cardarelli, M. DiLuca, F. Beltram, and E. Gratton, Biophys. J. **111**, 841 (2016).
[58]G. D. Dickinson, K. L. Ellefsen, S. P. Dawson, J. E. Pearson, and I. Parker, Sci. Signaling **9**, ra108 (2016).
[59]F. von Wegner, N. Wieder, and R. H. Fink, Front. Genet. **5**, 376 (2014).
[60]O. Krichevsky and G. Bonnet, Rep. Prog. Phys. **65**, 251 (2002).
[61]J. Wagner and J. Keizer, Biophys. J. **67**, 447 (1994).
[62]G. Smith, Biophys. J. **71**, 3064 (1996).
[63]A. Minta, J. P. Kao, and R. Y. Tsien, J. Biol. Chem. **264**, 8171 (1989).
[64]D. Qin, A. Yoshida, and A. Noma, Jpn. J. Physiol. **41**, 333 (1991).
[65]A. Gennerich and D. Schild, Biophys. J. **83**, 510 (2002).
[66]J. Shuai, H. J. Rose, and I. Parker, Biophys. J. **91**, 4033 (2006).
[67]C. T. Culbertson, S. C. Jacobson, and J. M. Ramsey, Talanta **56**, 365 (2002).
[68]F. Höffling and T. Franosch, Rep. Prog. Phys. **76**, 046602 (2013).
[69]L. Wawrezinieck, H. Rigneault, D. Marguet, and P.-F. Lenne, Biophys. J. **89**, 4029 (2005).
[70]P.-F. Lenne, L. Wawrezinieck, F. Conchonaud, O. Wurtz, A. Boned, X.-J. Guo, H. Rigneault, H.-T. He, and D. Marguet, EMBO J. **25**, 3245–3256 (2006).
[71]C. D. Rienzo, V. Piazza, E. Gratton, F. Beltram, and F. Cardarelli, Nat. Commun. **5**, 5891 (2014).
[72]MATLAB, version 7.10.0 (R2010a), The MathWorks, Inc., Natick, Massachusetts, 2010.
[73]P.-O. Gendron, F. Avaltroni, and K. Wilkinson, J. Fluoresc. **18**, 1093 (2008).